IEEE Access
Multidisciplinary | Rapid Review | Open Access Journal

Received April 9, 2020, accepted April 17, 2020, date of publication April 21, 2020, date of current version May 6, 2020.

Digital Object Identifier 10.1109/ACCESS.2020.2989299

Design and Characterization of Nanopore-Assisted Weakly-Coupled Few-Mode Fiber for Simpler MIMO Space Division Multiplexing

YUHENG XIE[1,2], LI PEI[1,2], JINGJING ZHENG[1,2], TIGANG NING[1,2], JING LI[1,2], BO AI[3], (Senior Member, IEEE), AND RUISI HE[3]

[1]Institute of Lightwave Technology, Beijing Jiaotong University, Beijing 100044, China
[2]Key Laboratory of all Optical Network and Advanced Telecommunication Network of Ministry of Education, Beijing Jiaotong University, Beijing 100044, China
[3]State Key Laboratory of Rail Traffic Control and Safety, Beijing Jiaotong University, Beijing 100044, China

Corresponding author: Li Pei (lipei@bjtu.edu.cn)

This work was supported in part by the National Key Research and Development Program of China under Grant 2018YFB1801003, in part by the National Natural Science Foundation of China (NSFC) under Grant 61827817 and Grant 61525501, and in part by the Fundamental Research Funds for the Central Universities under Grant 2019YJS001.

ABSTRACT We report on a novel weakly-coupled 6-LP-mode fiber that features a nanopore-assisted step-index core with double-cladding profile. The purpose of this fiber design is to alleviate modes coupling and bend sensitivity, thus simplifies the multiple-input multiple-output (MIMO) process and the environmental requirements in which the fiber is used. Through numerical simulations, we show that the minimum effective index difference (Δn_{eff}) of larger than $1.8*10^{-3}$ among all LP-mode over C and L band can be achieved by a simple nanopore with 170 nm radius in the center of the core. Furthermore, the dependences of both bending loss and chromatic dispersion on fiber structures are investigated by the finite element method (FEM) to show the good broadband performance. The proposed fiber targets applications in simpler MIMO space division multiplexing (SDM) systems such as data center and short-reach large-capacity transmission.

INDEX TERMS Few-mode fibers, mode coupling, nanopore-assisted, bending loss, dispersion.

I. INTRODUCTION

As a promising way to overcome capacity limitations of optical systems based on single-mode fibers (SMFs), space division multiplexing (SDM) transmission through multi-core fibers (MCFs) and few-mode fibers (FMFs) has attracted worldwide concern [1]–[5]. Compared with MCFs, FMF has the advantage of boosting the transmission capacity via a single enlarged core in the cladding. A variety of FMFs that support several modes have been investigated, which have different core parameters and structures [6]–[10].

Mode coupling is a major obstacle to the use of FMFs in SDM systems. Most FMF transmission experiments have been demonstrated using complex multiple-input multiple-output (MIMO) techniques to mitigate the random mode coupling, especially in long-haul transmissions [10]–[12]. Although the applying of graded-index fibers with minimal differential modal delay (DMD) is one of effective approaches, the 2M*2M equalizers are also necessary to separate all M spatial channels (each channel has two polarizations) for the higher-order LP modes. In contrast, in data centers, where direct detection is common, it is urgent to reduce the complexity of MIMO and decrease the number of operations and its power consumption. Weakly coupled fibers have the unique superiority. They reduce the dependence on MIMO process via minimizing mode coupling [13]–[15]. For a better understanding, each LP mode in weakly coupled fibers can be detected separately using simple 2*2 (non-degenerate LP modes) or 4*4 (two-time degenerate LP modes) MIMO technology, regardless of the number of modes. In this approach, signals can be transmitted and received independently, which makes the number of MIMO facilities decline dramatically.

Generally, simpler MIMO transmissions require that the degeneracy between spatial modes should be lifted. The effective index difference (Δn_{eff}) between adjacent LP modes should be larger than $1*10^{-3}$ [13]. Some efforts have been made to solve this problem. The high core-cladding index difference design was found to expand mode spacing. Yet, core-cladding index difference of more than 1.6% is needed

The associate editor coordinating the review of this manuscript and approving it for publication was San-Liang Lee.

to keep $\Delta n_{eff} = 1^{*}10^{-3}$ for a 6-LP-mode step-index fiber [1]. The special fiber structures, including ring-assisted cores, are introduced to increase the Δn_{eff} [6], [13], [16]–[18]. A latest record that the Δn_{eff} of higher than $1.49^{*}10^{-3}$ is achieved by a ring-core FMF with 6-LP-mode [13]. The fact is that the excessive changes in the core structure will alter fiber properties, such as transmission loss and increase the fabricating difficulty. Some elliptical cores are also designed to separate degenerate modes [9], [19], [20]. However, breaking the degeneracy usually brings an even smaller Δn_{eff}, which will restrict the number of independent modes. Besides, weakly coupled FMFs should be designed with other necessary properties. Random bending tends to occur in the actual fiber use, so the bending loss of FMFs has become one of the major concerns in its practical application [21]. The DMD and chromatic dispersion in FMFs should also be noted to keep stable signal transmission in the corresponding band. Therefore, a weakly coupled FMF should be designed with simple core structures and multiple spatial channels while suppressing mode coupling and bending loss.

In this paper, a novel nanopore-assisted 6-LP-mode fiber with double-cladding profile has been demonstrated to address the above issues. By the using of finite element method (FEM), COMSOL Multiphysics is adopted to simulate the mode field distribution and then the data are integrated to MATLAB for analyzing. Firstly, we introduce the design principle of weakly-coupled FMF and the nanopore-assisted core structure in section 2. It is revealed that, the minimum Δn_{eff} of larger than $1.8^{*}10^{-3}$ over C and L band can be achieved by a 170 nm-radius nanopore in the center of step-index core. Then, in order to understand the broadband performance of our designed fiber, the bending loss and chromatic dispersion dependences on fiber parameters and wavelengths are investigated in section 3. Finally, we clarify the fabrication tolerance and fiber properties. Through numerical simulations, we confirm that our proposed fiber shows great potential in the short-range large capacity simpler MIMO SDM systems.

II. PRINCIPLE AND NANOPORE-ASSISTED CORE DESIGN

A. DESIGN PRINCIPLE OF WEAKLY COUPLED FIBER

According to the coupled mode theory and power coupling theory, the mode coupling coefficient is inversely proportional to the Δn_{eff} [13], [22]. In the experiment of [23], there is a threshold of Δn_{eff} to describe the relationship between Δn_{eff} and the power coupling coefficient. When the Δn_{eff} is smaller than the threshold value, the power coupling coefficient decreases with increasing of Δn_{eff}. Yet, it changes insignificantly if Δn_{eff} is larger than that value.

It is found that the existing of lateral pressure and environmental fluctuation may lead to a larger threshold value of Δn_{eff}. Therefore, a fiber with large enough Δn_{eff} is expected to have better robustness to external fluctuation [6]. Researches show that to design a weakly-coupled FMF, sufficiently large Δn_{eff} between LP modes is essentially required. The minimum Δn_{eff} of larger than $1^{*}10^{-3}$ is the usual threshold for almost no modal-crosstalk [22]. Generally, the swept-wavelength interferometry technology is adopted to evaluate the inter-mode crosstalk. A former research indicate that when $\Delta n_{eff} \geq 0.8^{*}10^{-3}$, the power coupling coefficient for different modal vary from -29.8 dB/km to -22.7 dB/km in a ring-core 4-LP mode fiber, which is low enough to achieve weak coupling [6]. Thus, a FMF with the minimum $\Delta n_{eff} \geq 1^{*}10^{-3}$ can be considered as a weakly-coupled FMF.

Step-index core profiles have proven to be very well adapted to weakly coupled fibers. Fig. 1 shows, for this profile type, normalized propagation constant b as functions of normalized frequency V, where n_{eff} is the effective index of the LP mode, n_{co} is the index of core, n_{cl} is the index of cladding, r is the core radius, λ is the operating wavelength, taken here as 1550 nm. V and b are defined as (1) and (2), respectively [6]. The V number of 6.4 ensures robustness, supporting 6-LP modes and cutting off the next higher order modes. We can see that b of LP_{21} and LP_{02} is closest to each other, which means the minimum Δn_{eff} between them leads to the strongest mode crosstalk.

$$b = (n_{eff}^2 - n_{cl}^2)/(n_{co}^2 - n_{cl}^2) \tag{1}$$

$$V = 2\pi r\sqrt{n_{co}^2 - n_{cl}^2}/\lambda \tag{2}$$

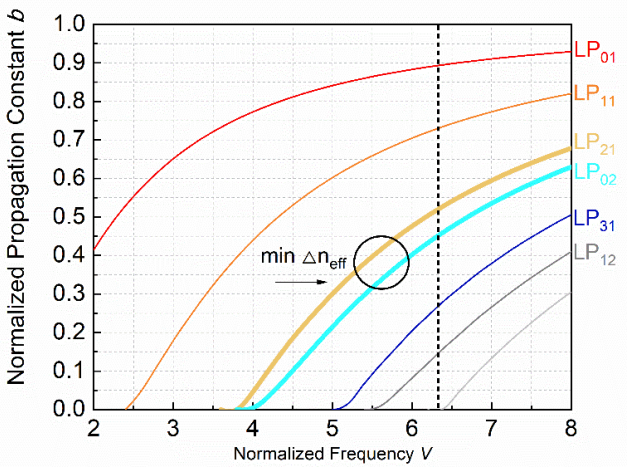

FIGURE 1. Normalized propagation constant b, versus normalized frequency V, for step-index core profiles.

To alleviate mode coupling, it is necessary to analyze the modes power distribution in step-index core. Figure 2 shows the normalized power distribution of 6 supporting modes along the normalized radial distance when $V = 6.4$. In theory, the n_{eff} of a LP mode can be manipulated by varying the refractive index of the corresponding core region in where the LP modes' most power distribute [13]. From Fig. 2, the field profiles of LP_{01} mode and LP_{02} mode have a maximum intensity at the center of core, while LP_{21} mode has its peak intensity in the middle area of the core. For a better understanding, any change of one's n_{eff} will have less of an effect on the other's. Therefore, adjusting the n_{eff} of a certain

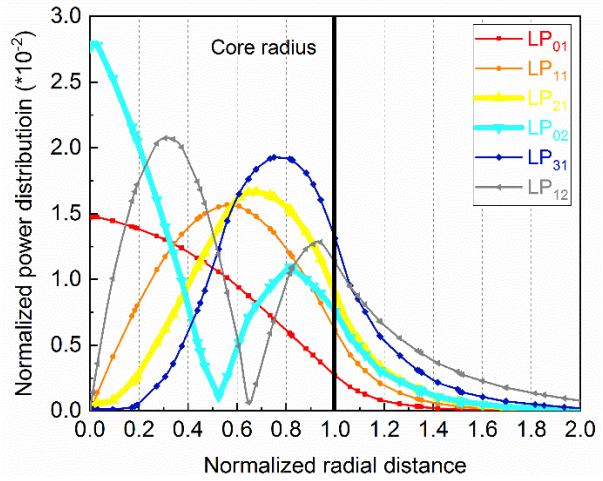

FIGURE 2. Normalized power distribution along the normalized radial distance when $V = 6.4$.

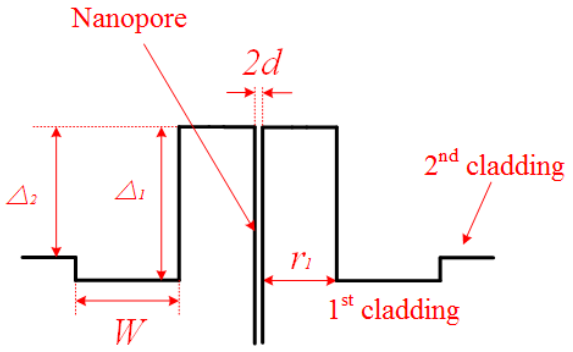

FIGURE 3. The index profile of nanopore-assisted double-cladding FMF design.

mode (or changing the position of its maximum power area) based on the step-index core profile is a simple and effective method for designing weakly-coupled FMFs. A large number of achievements have been obtained through this design theory. For instance, a modified ring-core design based on step-index core reduces the n_{eff} of LP_{02} through the low index region in the center of core [16] and another ring-assisted FMF design based on step-index core increase the n_{eff} of LP_{21} by inserting a high index ring [6]. In our consideration, the strategies of abandoning any mode or introducing additional ring structures are not adopted, since either of them will sacrifice mode amount or significantly change the core index profile and increase the manufacturing difficulty.

B. NANOPORE-ASSISTED CORE DESIGN

According to the design theory mentioned above, we demonstrate the design of an air hole with a nanometer width, which called nanopore, placed in the center of step-index core to modify overall mode spacing, since the nanopore has the lowest index so that it can sufficiently decrease the n_{eff} of LP_{02} and leaves no significant impact on other modes. The nanopore extends through the entire fiber lengths. Here, we set up a two-dimensional model through COMSOL Multiphysics to analyze the mode properties in FMFs. The frequency domain physics field under the wave optics module is selected. Figure 3 shows the index profile of the nanopore core design, where r_1, d, W are core radius, radius of nanopore and the width of 1st cladding, respectively. The influence of double-cladding structure will be discussed in section 3. The index contrast of core and cladding is defined as $\Delta_1 = (n_{co}^2 - n_{cl}^2)/(2n_{co}^2)$.

First, we need to select appropriate core parameters as the basic model. Considering 6 LP-mode transmission and the large space between the n_{eff} of the highest order mode and cladding index, $r_1 = 7.5\ \mu$m and $\Delta_1 = 1.0\%$ are set as the core parameters in terms of Eq. (2). In order to ensure the rigor and reliability of the calculation results, some preset parameters need to be arranged. To model the air hole with nano-scale sizes, the extremely-refined free-triangular divided meshes is used to improve the spatial resolution of the model. In addition, the amount of supporting modes as well as the operating wavelength are also should be considered in the modeling. To reveal the impact of the nanopore, the modal properties relative to nanopore parameters are calculated. Fig. 4 shows variation of the n_{eff} with d/r_1 at the wavelength $\lambda = 1550$ nm. The n_{eff} of LP_{01} and LP_{02} becomes small by the influence of nanopore, and it is reduced noticeably as d/r_1 grows large. Compared with LP_{01}'s, the n_{eff} of LP_{02} exhibits a more pronounced curvature. When d/r_1 is larger than 0.03, the n_{eff} of LP_{02} is approaching to that of LP_{31} sharply. In order to keep Δn_{eff} among all the modes large, the ratio of d/r_1 should range from 0.01 to 0.03.

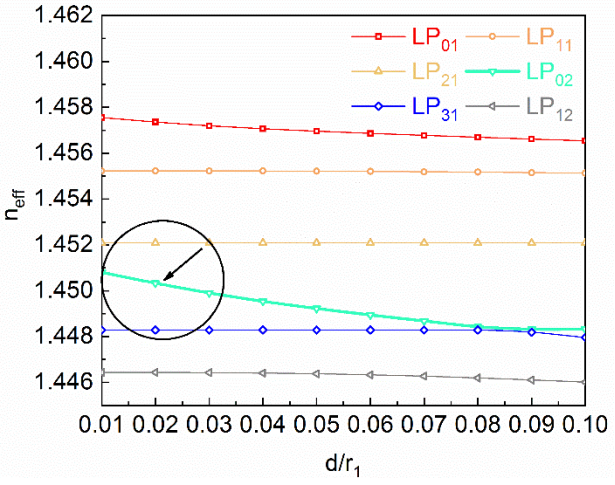

FIGURE 4. Variation of the n_{eff} with d/r_1 at the wavelength $\lambda = 1550$ nm.

Fig. 5 shows the Δn_{eff} of nanopore-assisted core as a function of d/r_1. In the shadowed area, Δn_{eff} among all the modes are larger than $1.85^{*}10^{-3}$ with d/r_1 ranging from 0.022 to 0.024, that is, $d = 165$ nm to $d = 180$ nm, as the design tolerance. We choose the point of $d/r_1 = 0.023$,

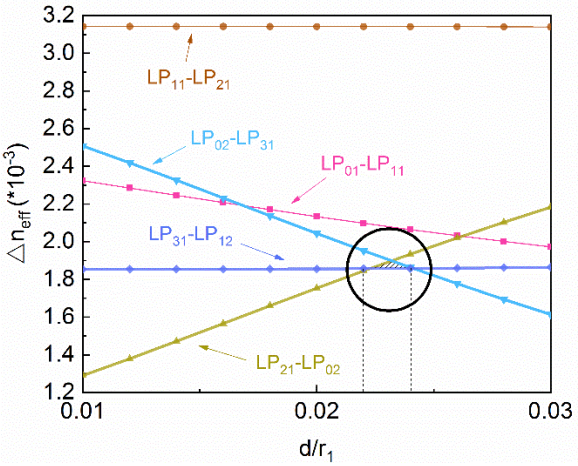

FIGURE 5. The Δn_{eff} of nanopore-assisted core as a function of d/r_1.

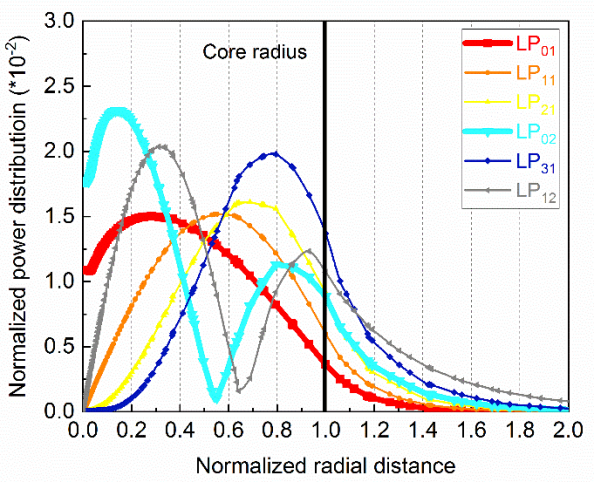

FIGURE 7. Normalized power distribution of nanopore-assisted core along the normalized radial distance.

that is, $d = 170$ nm, as the nanopore radius. The mode field distributions of LP modes in the nanopore-assisted core are shown in Fig. 6. It can be found that the nanopore is located at the most power area of LP_{01} and LP_{02}, which means the properties of other modes are hardly affected by this structure. Fig. 7 shows the normalized power distribution of nanopore-assisted core along the normalized radial distance. We find that the power of LP modes (except for LP_{01} and LP_{02}) in the nanopore-assisted core is almost unchanged in comparison to the normal step-index core. The most power area of LP_{01} and LP_{02} shift to the right with the existing of the nanopore. The results imply that the nanopore makes LP_{02} faces more power loss than LP_{01}, which is consistent with the change happened to their n_{eff} values in Fig. 4. The power change of some modes caused by nanopore is similar to the negative impact of ring-core or elliptical core structures. But the role that nanocore plays in suppressing mode coupling is what we should pay more attention to.

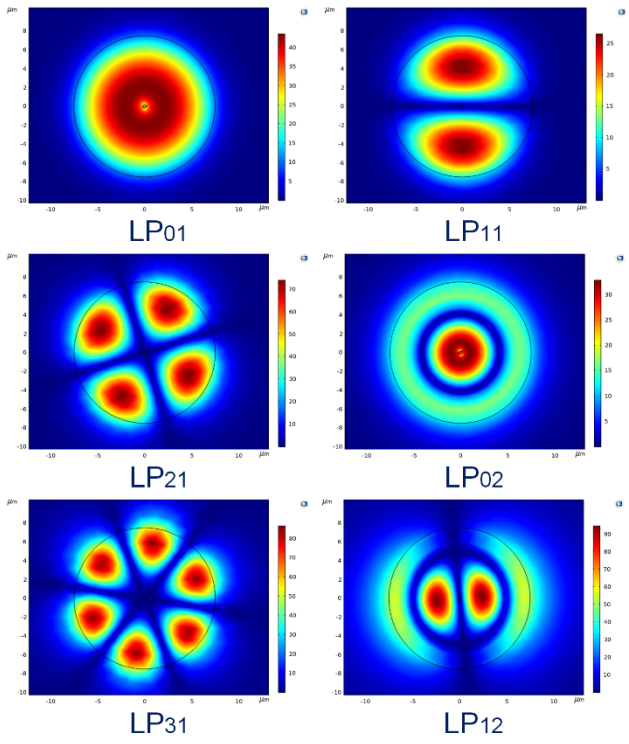

FIGURE 6. The mode field distributions of the LP modes in nanopore-assisted core profile.

The n_{eff} and Δn_{eff} of step-index core and nanopore-assisted core dependence on wavelength are calculated in Fig. 8. Fig. 8 (a) and (b) show the n_{eff} and Δn_{eff} of step-index core without nanopore corresponding to wavelength. The minimum Δn_{eff} of lower than $1*10^{-3}$ between LP_{21} and LP_{02} implies that the mode coupling may not be controlled into a desired value [22]. Furthermore, the n_{eff} and Δn_{eff} of nanopore-assisted core profile dependence on wavelength are presented in Fig. 8 (c) and (d). The designing core profile makes the Δn_{eff} of any neighbor mode of larger than $1.8*10^{-3}$ over the entire C+L band. Thus, if all the mode-groups are simultaneously used for dual-polarization SDM transmission, a relatively simple 2*2 and 4*4 MIMO is needed to recover the signals.

III. CHARACTERIZATION OF NANOPORE-ASSISTED FMF WITH DOUBLE-CLADDING STRUCTURE

A. FIBER PROPERTIES

The introduction of nanopore may change the fiber sensitivity on bending. To control this trend, a large piece of 1st cladding and a small piece of 2nd cladding with lower core-cladding index contrast are applied. The purpose of double-cladding design is to suppress the bending loss of guiding modes and increase the leakage loss of the unwanted higher-order mode in a limited cladding diameter. We evaluate the broadband characteristics of our proposed fiber over C and L band. Fig. 9 shows the schematic cross section of nanopore-assisted FMF with double-cladding structure.

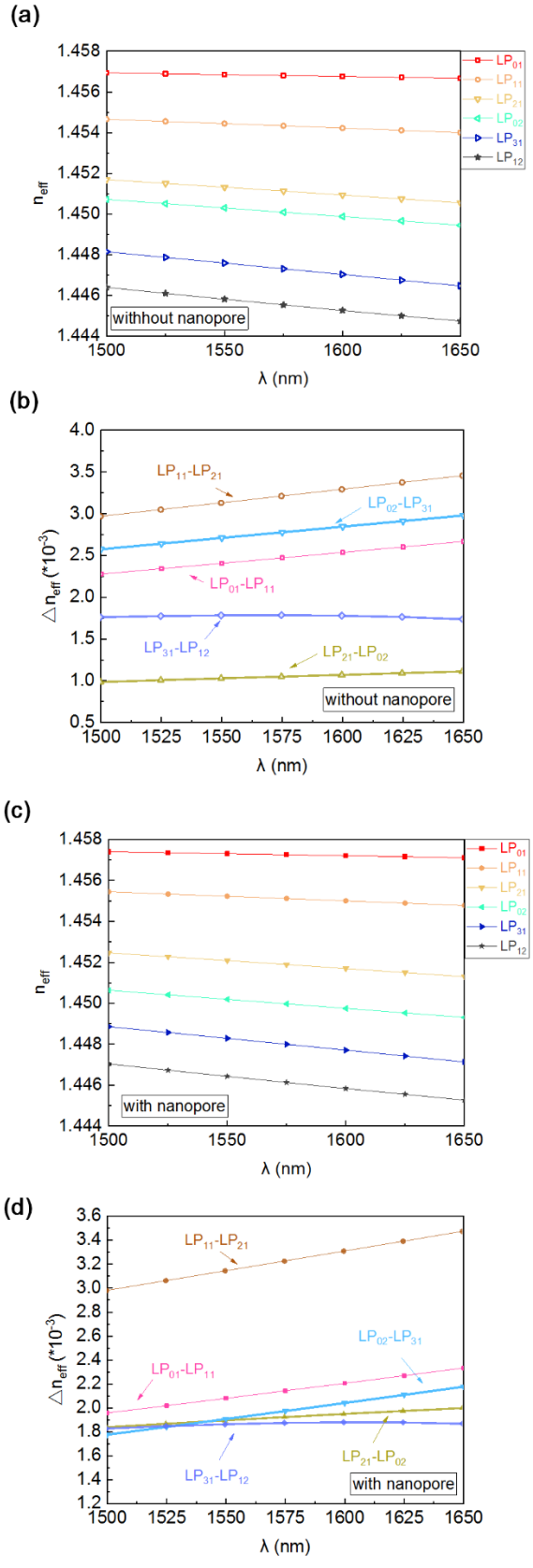

FIGURE 8. The (a) n_{eff} and (b) Δn_{eff} of step-index core dependence on wavelength; the (c) n_{eff} and (d) Δn_{eff} of nanopore-assisted core profile dependence on wavelength.

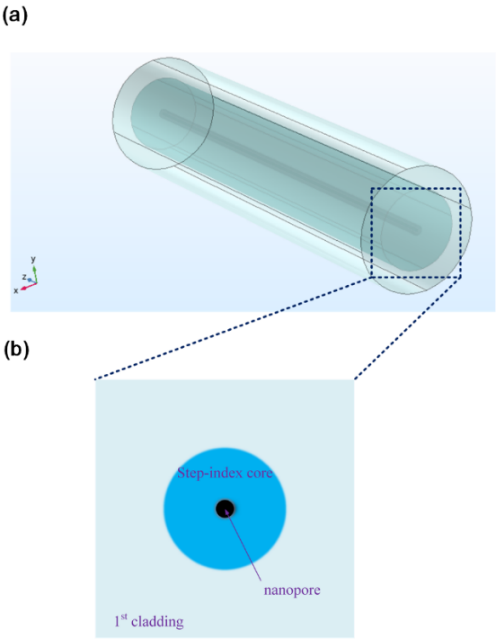

FIGURE 9. (a) Schematic cross section of nanopore-assisted double-cladding profile FMF and (b) detail of magnified core structure.

The 6-LP modes should be guaranteed to operate over C and L band. In reference to ITU-T recommendations G. 654, the bending loss should be lower than 0.5 dB/100 turns ($R_b = 30$ mm) for the highest-order mode (LP_{12}) at 1625 nm [24]. Furthermore, the bending loss of unwanted mode (LP_{41}) at 1530 nm ($R_b = 140$ mm) should be larger than 1 dB/m [24], [25]. In our modeling, a bent fiber is transformed into a straight fiber with equivalent refractive index method. Here, the perfect matching layer (PML) is necessary for calculating the characteristics of the bend fiber. Also, the bending radius and direction should be considered. The left bending direction along the x-axis is chosen in our simulation. The bending loss can be expressed by [21]:

$$BL = \frac{20}{\ln(10)} \frac{2\pi}{\lambda} imag(n_{eff}) \tag{3}$$

where $\mathrm{imag}(n_{eff})$ means the imaginary part of the n_{eff}.

The bending loss dependence on double-cladding parameters are calculated in Fig. 10. The solid and dashed lines correspond to the bending loss of LP_{12} after 100 turns at 1625 nm ($R_b = 30$ mm) and the bending loss of LP_{41} after 1-m transmission at 1530 nm ($R_b = 140$ mm), respectively. From Fig. 10 (a), $W > 18.2$ μm is needed to satisfy the demand of BL < 0.5 dB/100 turns of LP_{12}, while it should be smaller than 38 μm to keep bending loss of unwanted mode larger than 1 dB/m. In Fig. 10 (b), the Δ_2 of larger than 0.86% no longer meets the bending loss condition. Thus, the parameters of cladding can be determined, and the $W = 30$ μm and $\Delta_2 = 0.8\%$ is acceptable.

Specifically, the influence of fiber structure on chromatic dispersion should be noted. Chromatic dispersion of the transmission fibers is a major factor causing optical pulse

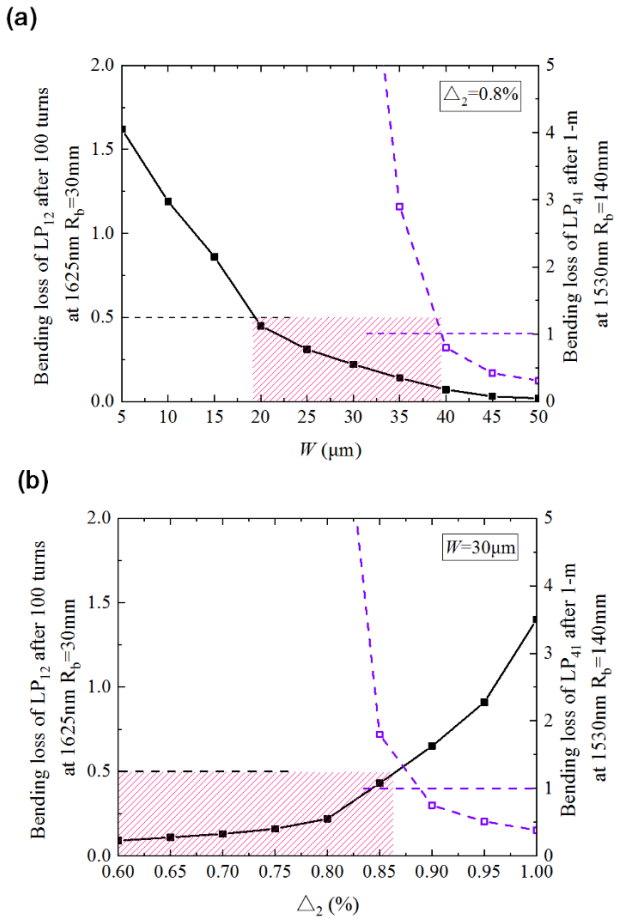

FIGURE 10. The bending loss dependence on (a) W and (b) Δ_2.

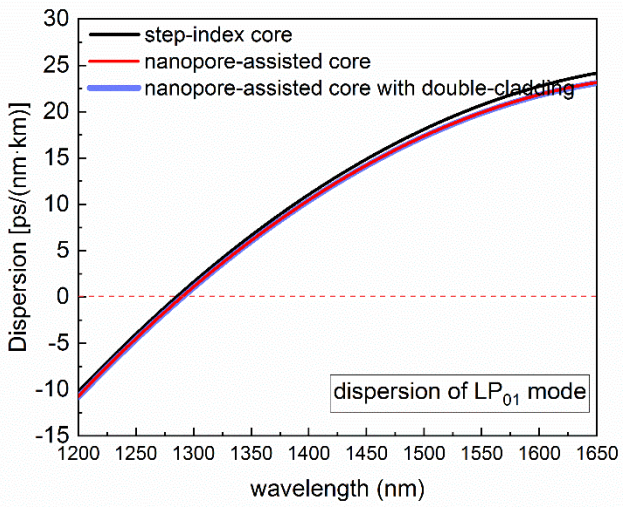

FIGURE 11. Dispersion of LP_{01} mode in the proposed fiber dependence on wavelength.

TABLE 1. The optimal fiber parameters with fabrication tolerance.

Symbol	Fiber parameters
r_1	7.5 μm
Δ_1	≥1.0%
Δ_2	≤0.8%
d	≤ 225 nm
W	30±10 μm
n_{cl}	1.444
CD	125μm

broadening [26]. The dispersion is composed of two components: material dispersion D_m and waveguide dispersion D_w, which can be written as Eq. (4), where c is the velocity of light in a vacuum, n_M is dependent on λ in dispersive media, $Re(n_{eff})$ is the real part of the n_{eff}, respectively.

$$\begin{aligned} D &= D_m + D_w \\ D_m &= -\frac{\partial^2 n_M}{\partial \lambda^2} \\ D_w &= -\left(\frac{\lambda}{c}\right)\frac{\partial^2 \mathrm{Re}\left(n_{eff}\right)}{\partial \lambda^2} \end{aligned} \tag{4}$$

Material dispersion refers to the wavelength dependence of the refractive index of material caused by the interaction between the optical modes and the state of material. The refractive indices of SiO_2 and GeO_2-SiO_2 at different wavelengths can be found in Refs. [26]. Waveguide dispersion depends among others on the fiber structure. The degree of effect of nanopore and double cladding on waveguide dispersion is an important part in determining the total dispersion. For example, we calculate the dispersion of LP_{01} mode in the proposed fiber dependence on wavelength in Fig. 11. As one can see, the slope of the dispersion curve of LP_{01} mode changes insignificantly with the added nanopore and double cladding structure. Definitely, we also calculate the dispersion of other higher-order modes along the wavelength. The simulation results indicate that the dispersion of higher-order modes follows the same trend as the fundamental mode. They are not varying too much on the entire C and L band in comparison to the dispersion values of the fiber without the nanopore and double-cladding structure. The chromatic dispersion values of these LP modes in our proposed fiber are summarized in Table 2.

Furthermore, the relationship between the A_{eff} and double-cladding parameters in nanopore-assisted core FMF is simulated in Fig. 12 (a) and (b), respectively. The A_{eff} of the propagation modes are approximately constant even if W and Δ_2 change, and they are larger than 110 μm^2. The DMD characteristics is important for the reduction of complexity and power consumption of MIMO processing. For example, the DMD between LP_{01} and LP_{11} can be defined as value that subtracted the group delay of LP_{01} from that of LP_{11} [16]. Figure 13 shows DMD of the proposed fiber dependence on wavelength. We find that the DMD increases slightly from short wavelength to the long wavelength. The broadband characteristics of the proposed fiber can reach the requirements of working in the C and L band.

TABLE 2. The optimal fiber performance of nanopore-assisted core double-cladding FMF.

	Fiber properties
n_{eff} at 1550 nm	1.4573 (LP_{01}), 1.4552 (LP_{11}),
	1.4520 (LP_{21}), 1.4501 (LP_{02})
	1.4482 (LP_{31}), 1.4464 (LP_{12})
$\Delta\ n_{eff}$ at C+L band	$\geq 1.8*10^{-3}$
Bending loss of LP_{12} mode at 1625 nm (R_b = 30 mm)	0.23 dB/100turns
Dispersion of LP modes at 1550 nm	20.1 (LP_{01}), 22.9 (LP_{11})
	24.7 (LP_{21}), 20.3 (LP_{02})
[ps/(nm·km)]	25.0 (LP_{31}), 26.2 (LP_{12})
A_{eff} at 1550 nm	129.65 μm^2 (LP_{01}), 158.07 μm^2 (LP_{11})
	166.40 μm^2 (LP_{21}), 111.77 μm^2 (LP_{02})
	169.46 μm^2 (LP_{31}), 147.89 μm^2 (LP_{12})
DMD at 1550 nm	-- ps/m (LP_{01}), 10.7 ps/m (LP_{11})
	21.5 ps/m (LP_{21}), 13.2 ps/m (LP_{02})
	30.3 ps/m (LP_{31}), 21.6 ps/m (LP_{12})

B. FABRICATION TOLERANCE ANALYSIS

It is very necessary to analyze the feasibility and manufacturing tolerance of the nanopore-assisted FMF with double-cladding structure in the actual fabricating process. The nano-level air holes are usually used in the development of micro-structured sensors [27], [28], probes [29] and the design of photonic crystal fibers [26], [30]–[32]. To the best of our knowledge, it is the first time that the nanopore has been applied to the FMFs in the transmission field.

As demonstrated above, the nanopore-assisted FMF with double-cladding structure features low mode coupling, low bending loss and large mode field area. However, it also has certain downsides. The obvious shortcoming is that the proposed fiber is not an all-solid structure, which means it has greater requirements on fabricating accuracy and difficulty than traditional fibers. Since the fiber structure is a simple combination of nanopore-assisted core and double-cladding, the main issues that are very likely to occur in the production are concentrated on the fabrication of the nanopore. One of them is the occlusion of the nanopore, and the other is the excessive nanopore diameter.

The problem of air holes occlusion sometimes appears in the fiber design of hole-assisted structure. The occlusion of air holes will affect the fiber performance to a certain extent. However, in our proposed fiber, the nanopore occlusion will only partially affect the modes coupling characteristics. Nonetheless, due to the pre-design of the high core-cladding contrast, the all-solid FMF caused by nanopore occlusion will make a limited effect on Δn_{eff} and it is acceptable, as shown in Fig. 8 (a) and (b).

On the other hand, an excessive nanopore diameter will also affect the fiber performance. As shown in Fig. 5,

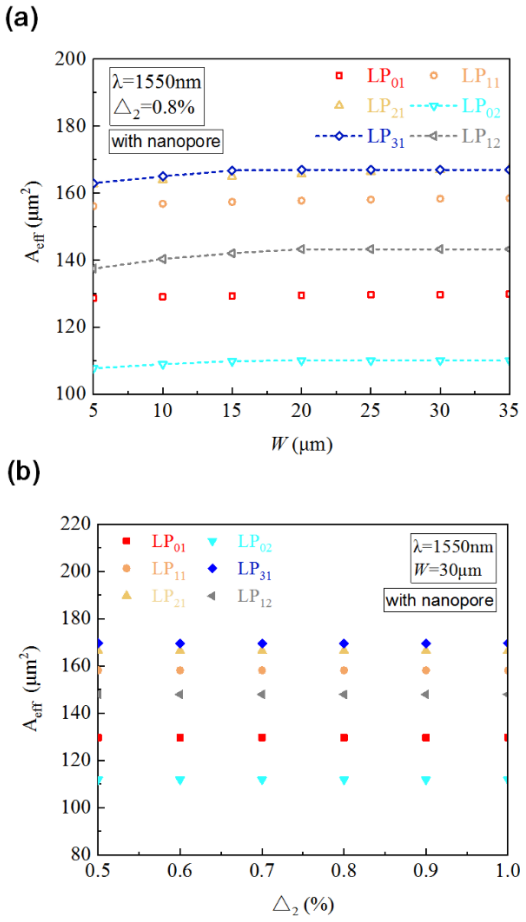

FIGURE 12. The A_{eff} of nanopore-assisted core FMF dependence on (a) W and (b) Δ_2 at 1550 nm.

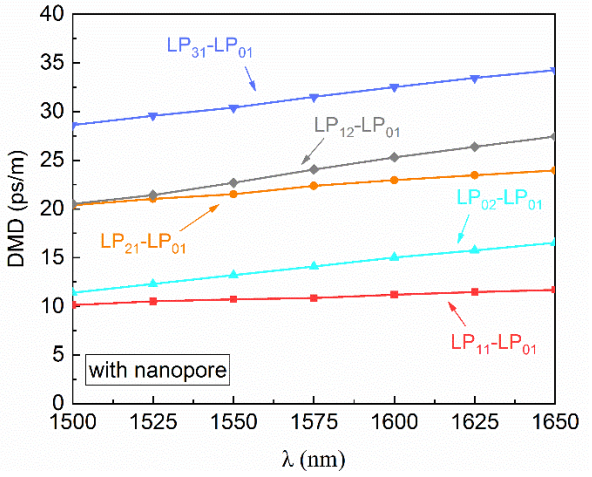

FIGURE 13. The DMD of the proposed fiber dependence on wavelength.

as d/r_1 continues to increase, the minimum Δn_{eff} between LP modes will reduce. When $d/r_1 = 0.03$, the lowest Δn_{eff} will become $1.6*10^{-3}$, which will sacrifice the weak coupling performance to some extent. Therefore, the tolerance of the d/r_1 should be less than 0.03, that is, $d \leq 225$ nm. If we

aimed at the best weak coupling performance, d should be set between 160 nm and 180 nm.

Choosing an appropriate fabricating method helps reduce the failure probability that may occur during the production. The stack-and-draw, which is a unique technology that can be used to fabricate micro-structured optical fiber via multiple glass rods and capillaries. This method is relatively mature and is widely used in making hole-assisted MCFs [33], photonic crystal fibers [30], [31] and segmented cladding fibers [34]. Figure 14 shows the schematic diagram of a stacked nanopore-assisted double-cladding structure FMF preform, where the GeO_2-doped preform is used to form the core, the glass rod can become the cladding and the glass capillary can shape the nanopore structure. After the above discussion, we believe that the design scheme of the nanopore-assisted double-cladding structure FMF is feasible, and the tolerance can meet the demand of the target broadband characteristics of the proposed fiber.

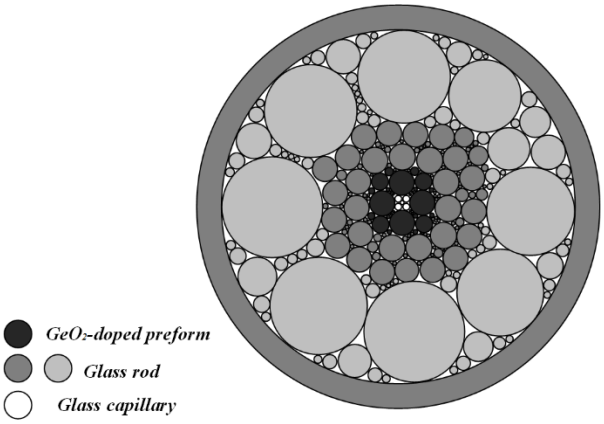

FIGURE 14. The schematic diagram of a stacked nanopore-assisted double-cladding structure FMF preform.

Finally, we summarize the optimal fiber parameters with fabrication tolerance and performance of our proposed fiber in Table 1 and Table 2, respectively. Simpler MIMO process will be adopted due to the ultra-high Δn_{eff} of larger than $1.8^{*}10^{-3}$ with nanopore-assisted core profile. The broadband characteristics have been optimized to maintain stable operation over the entire C and L band.

IV. CONCLUSION

We have proposed a nanopore-assisted core double-cladding profile 6-LP-mode fiber with ultra-high Δn_{eff} and optimized bending loss. By introducing a 170 nm-radius nanopore through the fiber length, the minimum Δn_{eff} between any two LP modes of larger than $1.8^{*}10^{-3}$ over C and L band can be achieved. The mode coupling and the complexity of MIMO process can be greatly reduced via this simple core structure. The broadband performances, including bending loss, dispersion and mode field area dependences on fiber parameters and structures are investigated. Through numerical simulations, we show that the nanopore has limited contribution to the changing of dispersion and the mode field area. Moreover, the bending loss are efficiently reduced by the double-cladding structure. The fabrication method and tolerance of the proposed fiber are illustrated. With the viewpoints of these properties, we believe that our designed fiber can be applied into simpler MIMO SDM systems in scenarios such as data center and computer rooms.

REFERENCES

[1] P. Sillard, M. Bigot-Astruc, and D. Molin, "Few-mode fibers for mode-division-multiplexed systems," *J. Lightw. Technol.*, vol. 32, no. 16, pp. 2824–2829, Aug. 15, 2014.
[2] Y. Jung, Q. Kang, H. Zhou, R. Zhang, S. Chen, H. Wang, Y. Yang, X. Jin, F. P. Payne, S.-U. Alam, and D. J. Richardson, "Low-loss 25.3 km few-mode ring-core fiber for mode-division multiplexed transmission," *J. Lightw. Technol.*, vol. 35, no. 8, pp. 1363–1368, Apr. 15, 2017.
[3] Y. Sasaki, "Few-mode multicore fiber with 36 spatial modes (three modes (LP_{01}, LP_{11a}, LP_{11b}) × 12 cores)," *J. Lightw. Technol.*, vol. 33, no. 5, pp. 964–970, Mar. 1, 2015.
[4] Y. Tobita, "Optimal design of 4LP-mode multicore fibers for high spatial multiplicity," *Optics Express*, vol. 25, no. 5, pp. 5697–5709, 2017.
[5] Y. Xie, L. Pei, J. Sun, J. Zheng, T. Ning, and J. Li, "Optimal design of a bend-insensitive heterogeneous MCF with differential inner-cladding structure and identical cores," *Opt. Fiber Technol.*, vol. 53, Dec. 2019, Art. no. 102001.
[6] S. Jiang, L. Ma, Z. Zhang, X. Xu, S. Wang, J. Du, C. Yang, W. Tong, and Z. He, "Design and characterization of ring-assisted few-mode fibers for weakly coupled mode-division multiplexing transmission," *J. Lightw. Technol.*, vol. 36, no. 23, pp. 5547–5555, Dec. 1, 2018.
[7] S. Fu, "Specialty few mode fiber and its application," in *Proc. Conf. Lasers Electro-Opt./Pacific Rim*. Washington, DC, USA: OSA, 2018, p. W4L-1.
[8] A. Gulistan, S. Ghosh, and B. M. A. Rahman, "Enhancement of modal stability through reduced mode coupling in a few-mode fiber for mode division multiplexing," *OSA Continuum*, vol. 1, no. 2, pp. 309–319, Oct. 2018.
[9] J. Liang, Q. Mo, S. Fu, M. Tang, P. Shum, and D. Liu, "Design and fabrication of elliptical-core few-mode fiber for MIMO-less data transmission," *Opt. Lett.*, vol. 41, no. 13, pp. 3058–3061, Jul. 2016.
[10] T. Mori, "Few-mode fibers supporting more than two LP modes for mode-division-multiplexed transmission with MIMO DSP," *J. Lightw. Technol.*, vol. 32, no. 14, pp. 2468–2479, Jul. 15, 2014.
[11] T. Sakamoto, T. Matsui, K. Saitoh, S. Saitoh, K. Takenaga, T. Mizuno, Y. Abe, K. Shibahara, Y. Tobita, S. Matsuo, K. Aikawa, S. Aozasa, K. Nakajima, and Y. Miyamoto, "Low-loss and low-DMD 6-Mode 19-core fiber with cladding diameter of less than 250 μm," *J. Lightw. Technol.*, vol. 35, no. 3, pp. 443–449, Feb. 1, 2017.
[12] K. Shibahara, "Dense SDM (12-Core 3-Mode) transmission over 527 km with 33.2-ns mode-dispersion employing low-complexity parallel MIMO frequency-domain equalization," *J. Lightw. Technol.*, vol. 34, no. 1, pp. 196–204, Jan. 1, 2016.
[13] D. Ge, J. Li, J. Zhu, L. Shen, Y. Gao, J. Yu, Z. Wu, Z. Li, Z. Chen, and Y. He, "Design of a weakly-coupled ring-core FMF and demonstration of 6-mode 10-km IM/DD transmission," in *Proc. Opt. Fiber Commun. Conf.* San Diego, CA, USA: Optical Society of America, 2018.
[14] L. Shen, S. Chen, X. Sun, Y. Liu, L. Zhang, T. Hu, and J. Li, "Design, fabrication, measurement and MDM tranmission of a novel weakly-coupled ultra low loss FMF," in *Proc. Opt. Fiber Commun. Conf.* Washington, DC, USA: OSA, Mar. 2018, p. Th2A-24.
[15] T. Hu, J. Li, D. Ge, Z. Wu, Y. Tian, L. Shen, Y. Liu, S. Chen, Z. Li, Y. He, and Z. Chen, "Weakly-coupled 4-mode step-index FMF and demonstration of IM/DD MDM transmission," *Opt. Express*, vol. 26, no. 7, pp. 8356–8363, Apr. 2018.
[16] M. Kasahara, K. Saitoh, T. Sakamoto, N. Hanzawa, T. Matsui, K. Tsujikawa, and F. Yamamoto, "Design of three-spatial-mode ring-core fiber," *J. Lightw. Technol.*, vol. 32, no. 7, pp. 1337–1343, Apr. 5, 2014.
[17] H. Yan, S. Li, Z. Xie, X. Zheng, H. Zhang, and B. Zhou, "Design of PANDA ring-core fiber with 10 polarization-maintaining modes," *Photon. Res.*, vol. 5, no. 1, pp. 1–5, Feb. 2017.
[18] Y. Xie, L. Pei, J. Zheng, Q. Zhao, T. Ning, and J. Sun, "Design and analysis of a combined-ring core weakly coupled few-mode fiber with six linearly polarized modes and an ultra-large effective index difference," *Appl. Opt.*, vol. 58, no. 16, pp. 4373–4380, Jun. 2019.

[19] F. Ren, "Design of 20-polarization-maintaining-mode 'pseudo-rectangle' elliptical-core fiber for MIMO-less MDM networks," *Opt. Fiber Technol.*, vol. 50, pp. 87–94, Jul. 2019.
[20] H. Xiao, H. Li, B. Wu, Y. Dong, S. Xiao, and S. Jian, "Elliptical hollow-core optical fibers for polarization-maintaining few-mode guidance," *Opt. Fiber Technol.*, vol. 48, pp. 7–11, Mar. 2019.
[21] X. Zheng, G. Ren, L. Huang, H. Li, B. Zhu, H. Zheng, and M. Cao, "Bending losses of trench-assisted few-mode optical fibers," *Appl. Opt.*, vol. 55, no. 10, pp. 2639–2648, Apr. 2016.
[22] J. Li, Z. Wu, T. Hu, D. Ge, Y. Tian, Y. Zhang, L. Shen, Y. Liu, S. Chen, Z. Li, Z. Chen, and Y. He, "Weakly-coupled mode-division-multiplexing systems and networks supporting large quantity of independent modes," in *Proc. 16th Int. Conf. Opt. Commun. Netw. (ICOCN)*, Aug. 2017, pp. 1–3.
[23] R. Maruyama, N. Kuwaki, S. Matsuo, and M. Ohashi, "Relationship between mode coupling and fiber characteristics in few-mode fibers analyzed using impulse response measurements technique," *J. Lightw. Technol.*, vol. 35, no. 4, pp. 650–657, Feb. 15, 2017.
[24] *Characteristics of a Cut-Off Shifted, Single-Mode Optical Fibre and Cable*, document ITU-T G.654, ITU_T Recommendation, Jul. 2010. [Online]. Available: https://www.itu.int/rec/T-REC-G.654-201007-S/en
[25] J. H. Chang, "Heterogeneous 12-core 4-LP-mode fiber based on trench-assisted graded-index profile," *IEEE Photonics J.*, vol. 9, no. 2, pp. 1–10, Mar. 2017.
[26] S. Haxha and H. Ademgil, "Novel design of photonic crystal fibres with low confinement losses, nearly zero ultra-flatted chromatic dispersion, negative chromatic dispersion and improved effective mode area," *Opt. Commun.*, vol. 281, no. 2, pp. 278–286, Jan. 2008.
[27] B. Delobelle, D. Perreux, and P. Delobelle, "Failure of nano-structured optical fibers by femtosecond laser procedure as a strain safety-fuse sensor for composite material applications," *Sens. Actuators A, Phys.*, vol. 210, pp. 67–76, Apr. 2014.
[28] K. Schaarschmidt, S. Weidlich, D. Reul, and M. A. Schmidt, "Bending losses and modal properties of nano-bore optical fibers," *Opt. Lett.*, vol. 43, no. 17, pp. 4192–4195, Sep. 2018.
[29] C. M. Rollinson, S. T. Huntington, B. C. Gibson, S. Rubanov, and J. Canning, "Characterization of nanoscale features in tapered fractal and photonic crystal fibers," *Opt. Express*, vol. 19, no. 3, pp. 1860–1865, Jan. 2011.
[30] D. Xu, T. Chen, K. Chen, H. Wang, Y. Lu, and Y. Lin, "Laser-assisted chemical vapor deposition of silicon nano-layers in air-hole microstructure fibers," in *Proc. Conf. Lasers Electro-Opt.*, San Jose, CA, USA: Optical Society of America, 2010, pp. 1–2.
[31] S. Huntington, J. Katsifolis, B. Gibson, J. Canning, K. Lyytikainen, J. Zagari, L. Cahill, and J. Love, "Retaining and characterising nano-structure within tapered air-silica structured optical fibers," *Opt. Express*, vol. 11, no. 2, pp. 98–104, Jan. 2003.
[32] B. C. Gibson, S. T. Huntington, S. Rubanov, P. Olivero, K. Digweed-Lyytikäinen, J. Canning, and J. D. Love, "Exposure and characterization of nano-structured hole arrays in tapered photonic crystal fibers using a combined FIB/SEM technique," *Opt. Express*, vol. 13, no. 22, pp. 9023–9028, Oct. 2005.
[33] A. Ziolowicz, M. Szymanski, L. Szostkiewicz, T. Tenderenda, M. Napierala, M. Murawski, Z. Holdynski, L. Ostrowski, P. Mergo, K. Poturaj, M. Makara, M. Slowikowski, K. Pawlik, T. Stanczyk, K. Stepien, K. Wysokinski, M. Broczkowska, and T. Nasilowski, "Hole-assisted multicore optical fiber for next generation telecom transmission systems," *Appl. Phys. Lett.*, vol. 105, no. 8, Aug. 2014, Art. no. 081106.
[34] S. Ma, T. Ning, L. Pei, J. Li, and J. Zheng, "Bend-resistant large mode area fiber with novel segmented cladding," *Opt. Laser Technol.*, vol. 98, pp. 113–120, Jan. 2018.

YUHENG XIE was born in Shenyang, China, in 1993. He is currently pursuing the Ph.D. degree in communication and information system with Beijing Jiaotong University, Beijing, China. His current research interests include special fiber design, optical fiber sensor, and novel optical devices.

LI PEI was born in Shanxi, China. She is currently a Professor with the School of Electronics and Information Engineering, Beijing Jiaotong University, Beijing, China. Her current research interests include high-speed optical telecommunication networks, optical fiber sensor, radio-over-fiber communication systems, and novel optical devices.

JINGJING ZHENG was born in Henan, China. She is currently an Associate Professor with the School of Electronics and Information Engineering, Beijing Jiaotong University, Beijing, China. Her current research interests include specialty fiber and components, optical fiber sensor, and novel optical devices.

TIGANG NING received the Ph.D. degree in telecommunication and information system from Northern Jiaotong University, Beijing, China, in 2003. He is currently a Professor with the School of Electronics and Information Engineering, Beijing Jiaotong University. His recent research interests include all-optical networking, high-power fiber laser, and radio-over-fiber communication systems.

JING LI received the B.E. degree in communication engineering form the People's Liberation Army, Academy of Communication and Commanding, Wuhan, China, in 2006, the M.E. degree in electromagnetic field and microwave technology form the Communication University of China, Beijing, China, in 2008, and the Ph.D. degree in communication and information system from Beijing Jiaotong University, Beijing, in 2013. His research interests are microwave photonic generator and radio-over-fiber communication systems.

BO AI (Senior Member, IEEE) received the Ph.D. degree in telecommunication and information system from Xidian University, Beijing, China, in 2004. He is currently a Professor with the Key Laboratory of all Optical Network and Advanced Telecommunication Network of Ministry of Education, Beijing Jiaotong University, Beijing. His recent research interests include broadband mobile communication systems and dedicated mobile communications.

RUISI HE received the Ph.D. degree from Beijing Jiaotong University, Beijing, China, in 2015. He is currently a Professor with the Key Laboratory of all Optical Network and Advanced Telecommunication Network of Ministry of Education, Beijing Jiaotong University. His recent research interests include broadband mobile communication systems and dedicated mobile communications.